

Adsorption of propylene carbonate on the $LiMn_2O_4$ (100) surface investigated by DFT + *U* calculations

Wei Hu(胡伟), Wenwei Luo(罗文崴), Hewen Wang(王鹤文), and Chuying Ouyang(欧阳楚英)

Citation: Chin. Phys. B, 2021, 30 (**3**): 038202. DOI: 10.1088/1674-1056/abd77e
Journal homepage: http://cpb.iphy.ac.cn; http://iopscience.iop.org/cpb

What follows is a list of articles you may be interested in

DFT study of solvation of Li^+/Na^+ in fluoroethylene carbonate/vinylene carbonate/ethylene sulfite solvents for lithium/sodium-based battery

Qi Liu(刘琦), Guoqiang Tan(谭国强), Feng Wu(吴锋), Daobin Mu(穆道斌), and Borong Wu(吴伯荣)
Chin. Phys. B, 2021, 30 (**3**): 038203. DOI: 10.1088/1674-1056/abd763

Suppressing transition metal dissolution and deposition in lithium-ion batteries using oxide solid electrolyte coated polymer separator

Zhao Yan(闫昭), Hongyi Pan(潘弘毅), Junyang Wang(汪君洋), Rusong Chen(陈汝颂), Fei Luo(罗飞), Xiqian Yu(禹习谦), Hong Li(李泓)
Chin. Phys. B, 2020, 29 (**8**): 088201. DOI: 10.1088/1674-1056/ab9610

Influence of fluoroethylene carbonate on the solid electrolyte interphase of silicon anode for Li-ion batteries: A scanning force spectroscopy study

Jieyun Zheng(郑杰允), Jialiang Liu(刘家亮), Suijun Wang(王绥军), Fei Luo(罗飞), Liubin Ben(贲留斌), Hong Li(李泓)
Chin. Phys. B, 2020, 29 (**4**): 048203. DOI: 10.1088/1674-1056/ab7b54

Comparative calculation on Li^+ solvation in common organic electrolyte solvents for lithium ion batteries

Qi Liu(刘琦), Feng Wu(吴锋), Daobin Mu(穆道斌), Borong Wu(吴伯荣)
Chin. Phys. B, 2020, 29 (**4**): 048202. DOI: 10.1088/1674-1056/ab75cc

Failure analysis with a focus on thermal aspect towards developing safer Na-ion batteries

Yuqi Li(李钰琦), Yaxiang Lu(陆雅翔), Liquan Chen(陈立泉), Yong-Sheng Hu(胡勇胜)
Chin. Phys. B, 2020, 29 (**4**): 048201. DOI: 10.1088/1674-1056/ab7906

Adsorption of propylene carbonate on the $LiMn_2O_4$ (100) surface investigated by DFT + U calculations*

Wei Hu(胡伟)[1], Wenwei Luo(罗文崴)[1,†], Hewen Wang(王鹤文)[2], and Chuying Ouyang(欧阳楚英)[1]

[1] *Department of Physics, Laboratory of Computational Materials Physics, Jiangxi Normal University, Nanchang* 330022, *China*
[2] *College of Chemistry and Chemical Engineering, Hubei Key Laboratory for Processing and Application of Catalytic Materials, Huanggang Normal University, Huanggang* 438000, *China*

(Received 20 October 2020; revised manuscript received 24 November 2020; accepted manuscript online 30 December 2020)

Understanding the mechanism of the interfacial reaction between the cathode material and the electrolyte is a significant work because the interfacial reaction is an important factor affecting the stability, capacity, and cycling performance of Li-ion batteries. In this work, spin-polarized density functional theory calculations with on-site Coulomb energy have been employed to study the adsorption of electrolyte components propylene carbonate (PC) on the $LiMn_2O_4$ (100) surface. The findings show that the PC molecule prefers to interact with the Mn atom on the $LiMn_2O_4$ (100) surface via the carbonyl oxygen (O_c), with the adsorption energy of -1.16 eV, which is an exothermic reaction. As the adsorption of organic molecule PC increases the Mn atoms coordination with O atoms on the (100) surface, the Mn^{3+} ions on the surface lose charge and the reactivity is substantially decreased, which improves the stability of the surface and benefits the cycling performance.

Keywords: Li-ions batteries, electrolyte, density functional theory, surface, propylene carbonate

PACS: 82.47.Aa, 81.05.Hd, 82.20.Ej **DOI:** 10.1088/1674-1056/abd77e

1. Introduction

Li-ion batteries have received significant attention due to their high energy density and environmental friendliness, and are widely used as energy storage devices of small electronic products and electric vehicles. Currently, the research and development of Li-ion batteries mainly focus on improving the performance of existing battery systems and developing new battery materials to achieve specific applications.[1,2] In the Li-ion batteries system, the cathode material, as a provider of Li-ions, plays a key role in the electrochemical performance of the battery,[3–5] regarding safety, price, capacity, etc. Different types of cathode materials have been considered for Li-ion batteries, including layered structured materials $LiMO_2$ (M = Co, Ni, Mn),[6–11] spinel structured material $LiMn_2O_4$,[12–15] Li-rich material Li_2MnO_3,[16–18] and olivine structured material $LiFePO_4$.[19–22] Among these materials, spinel $LiMn_2O_4$ has attracted much attention because of the following advantages: (i) manganese is low-priced, abundant; (ii) $LiMn_2O_4$ shows high working voltage with a theoretical capacity of 148 mAh/g; (iii) $LiMn_2O_4$ has a three-dimensional channel for the reversible diffusion of Li^+ ions.[23,24]

However, $LiMn_2O_4$ also shows some undesirable features as a positive electrode, such as disproportionated reaction and Jahn–Teller distortion of Mn^{3+} ion.[14,25,26] Doping and surface coating are considered to be effective methods to improve the battery performance. Zhang *et al.*[25] found that Al/Co dual-doped $LiMn_2O_4$ showed a good cycling stability. Ouyang *et al.*[15] pointed out that Al_2O_3-covered $LiMn_2O_4$ (100) surface inhibited the formation of Mn^{3+} ions. Although some progress has been achieved in the investigation of $LiMn_2O_4$, there are still problems to be solved in order to further improve the electrochemical performance of $LiMn_2O_4$,[27–29] such as severe capacity degradation at high temperatures, interfacial reaction, etc.

In the present work, we studied the interfacial reaction of propylene carbonate $C_4H_6O_3$ (PC) on the $LiMn_2O_4$ (100) surface and proposed the corresponding reaction mechanism with the help of density functional theory (DFT) calculations. The results provide a theoretical explanation to the better cycling performance of PC based electrolyte for the $LiMn_2O_4$ cathodes.

2. Computational details

All calculations of interfacial reaction were performed using the projector augmented wave (PAW) method based on DFT+U calculations as implemented in the Vienna *ab initio* simulation package (VASP) code.[30–32] The exchange–correlation functional was modeled using the Perdew, Burke, and Ernzerhof (PBE) within the spin-polarized generalized gradient approximation (GGA). The plane wave cut-off energy of 520 eV and k sampling with $3 \times 3 \times 1$ k-point mesh in Brillouin zone were adopted for all surface adsorption models. Li-$2s^1$, C-$2s^2 2p^2$, H-$1s^1$, Mn-$3d^6 4s^1$, and O-$2s^2 2p^4$ were modeled as valence electrons. The Hubbard U correction term

*Project supported by the National Natural Science Foundation of China (Grant No. 51962010).
†Corresponding author. E-mail: luowenwei@jxnu.edu.cn
© 2021 Chinese Physical Society and IOP Publishing Ltd

was used to improve the description of the localized Mn-3d electrons.[33] The on-site U parameter for the Mn-3d electrons was set to be 4.5 eV based on previous study.[34]

In order to characterize the adsorption strength of PC molecule on $LiMn_2O_4$ (100) surface, we calculated the adsorption energy (E_{ads}) at different adsorption sites with different orientations on the molecule. The adsorption energy was calculated according to the following equation:

$$E_{ads} = E_{total} - E_{slab} - E_{PC},$$

where E_{total} represents the total energy of the slab after adsorbing molecules, E_{slab} and E_{PC} are the energies of the clean slab and the isolated PC molecule, respectively. A negative value of E_{ads} corresponds to an exothermic and favorable absorption process. The larger the negative value is, the more stable the adsorption is.

3. Results and discussion

The spinel $LiMn_2O_4$ has a cubic crystal structure with space group Fdm, and the structural model is shown in Fig. 1. Li-ion occupies the 8a tetrahedral sites, Mn-ion occupies the 16d octahedral sites, and O-ion occupies the 32e sites. Mn is present as Mn^{3+} and Mn^{4+} ions in $LiMn_2O_4$ bulk,[15,35] i.e., 8 Mn^{3+} and 8 Mn^{4+}. Mn^{3+} corresponds to the $t_{2g}^3e_g^1$ electronic configuration, and Mn^{4+} is consistent with t_{2g}^3 electronic configuration. According to the ligand field theory, there is a single un-paired electron in d_{z^2} component of the e_g orbitals for the Mn^{3+} ion, the Mn–O bond is elongated along the z direction, resulting in the so called Jahn–Teller distortion. Mn^{3+} is largely responsible for the structural instability of the spinel $LiMn_2O_4$ cathode material.

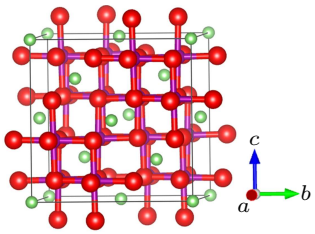


Fig. 1. The structural model of the spinel $LiMn_2O_4$. The green, purple, and red balls are Li, Mn, and O atoms, respectively.

For low index surfaces of spinel $LiMn_2O_4$, previous studies have pointed out that the Li-terminated $LiMn_2O_4$ (100) surface is the energetically most favorable surface,[15,28] as shown in Fig. 2(a). The Mn atoms in the $LiMn_2O_4$ (100) surface only coordinate with 5 O atoms, the d_{z^2} orbital is filled with electrons. Therefore, all Mn ions in the $LiMn_2O_4$ (100) surface are present in the form of Mn^{3+}. Researches show that the Mn^{3+} ions are easier to dissolve in the electrolyte than the Mn^{4+} ions,[15,36] which is now considered to be an important cause of performance fading. In the present work, the interfacial reaction between the $LiMn_2O_4$ (100) surface and the PC molecule is studied, the structural models are shown in Fig. 2. To avoid the interaction between the periodic images, a vacuum layer of 15 Å along c axis was added to the (100) surface. The initial adsorption configuration of the PC molecule involved coordination with the surface via the carbonyl (O_c) and ethereal (O_e) oxygens, and the adsorption positions studied included top-Li, top-Mn, and bridge-Mn sites, as shown in Fig. 3. Various adsorption configurations and corresponding adsorption energies E_{ads} are presented in Table 1. It can be clearly found that all the adsorption energies are negative. This indicates that the adsorption of PC molecule on the $LiMn_2O_4$ (100) surface is an exothermic reaction that can occur spontaneously. For the monodentate binding pattern (sites A to F), the adsorption energy of PC via O_c adsorption is greater than that via O_e adsorption at the same site. The top-Mn site is the favorite adsorption site, while the bridge-Mn is the opposite. For the bidentate adsorption pattern, the case which interacts with surface Mn atoms via O_c and one O_e has the adsorption energy of -0.90 eV, while the adsorption energy of interaction with surface Mn atoms via two O_e is only -0.42 eV. The adsorption energy of the out-of-plane adsorption pattern via H atoms (site I) is the smallest. Therefore, we can conclude that the PC molecule prefers to interact with the Mn atom on the $LiMn_2O_4$ (100) surface via O_c (site C) at a distance of 2.646 Å, with the adsorption energy of -1.16 eV, as shown in Fig. 4. Hence the adsorption pattern which interacts with the surface Mn atoms via O_c will be further studied due to more negative adsorption energy.

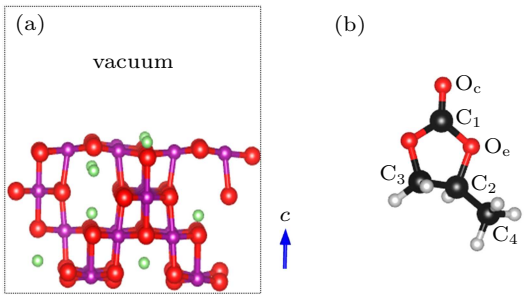


Fig. 2. Structural models of (a) $LiMn_2O_4$ (100) surface and (b) propylene carbonate $C_4H_6O_3$ (PC) molecule. The green, purple, black, gray, and red balls are Li, Mn, C, H, and O atoms, respectively. O_c and O_e represent the carbonyl and ethereal oxygens, respectively. C_1–C_4 is the code for the C atom.

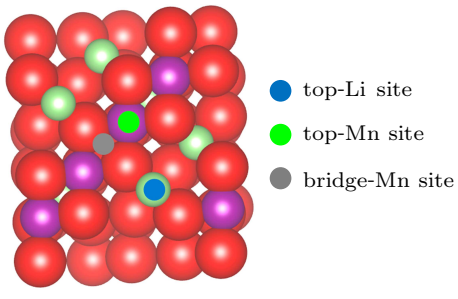
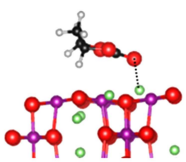
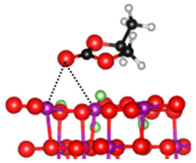
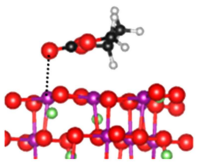
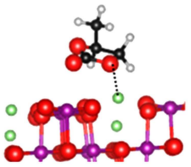
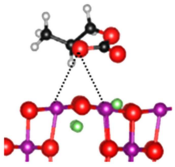
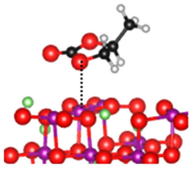
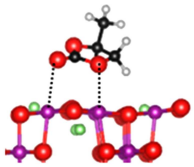
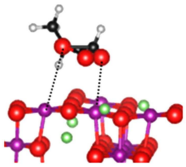
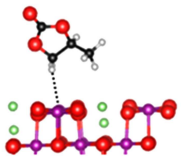


Fig. 3. Schematic diagram of adsorption sites on $LiMn_2O_4$ (100) surface. The green, purple, and red balls are Li, Mn, and O atoms, respectively.

Table 1. Various adsorption configurations and corresponding adsorption energy E_{ads} of PC adsorbed on $LiMn_2O_4$ (100) surface. The green, purple, black, gray, and red balls are Li, Mn, C, H, and O atoms, respectively.

Site	A	B	C
Adsorption configuration			
E_{ads} (eV)	−0.82	−0.59	−1.16
Site	D	E	F
Adsorption configuration			
E_{ads} (eV)	−0.70	−0.40	−1.05
Site	G	H	I
Adsorption configuration			
E_{ads} (eV)	−0.90	−0.42	−0.23

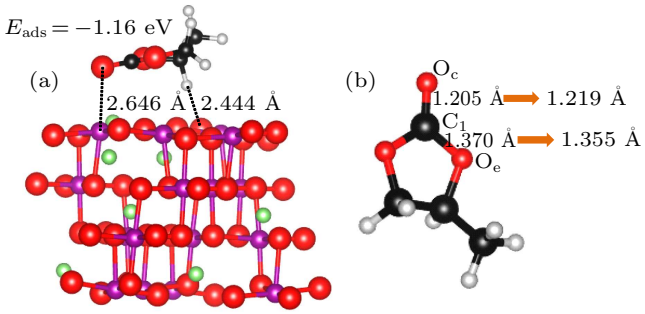


Fig. 4. Most stable adsorption configurations for the PC molecule on the $LiMn_2O_4$ (100) surface (a) and structural changes of PC molecule after adsorption (b). The green, purple, black, gray, and red balls are Li, Mn, C, H, and O atoms, respectively.

In order to gain an insight into the reaction mechanism, the differential charge density $\rho_{diff} = \rho_{total} - \rho_{surface} - \rho_{PC}$ (ρ_{total}, $\rho_{surface}$, and ρ_{PC} represent the charge densities of total, surface, and isolated PC molecules, respectively) was first studied, as shown in Fig. 5. It can be clearly seen that there is an obvious charge transfer between Mn and carbonyl oxygen. Mn is the donor of electrons and oxygen is the acceptor of electrons. At the same time, the electron density aggregation between C_1 and ethereal oxygen (O_e), and between H and one surface O is observed, indicating that the interaction between these atoms becomes stronger. After the PC molecule is adsorbed on the (100) surface, the C_1–O_c bond length is stretched from 1.205 Å to 1.219 Å, while the C_1–O_e bond length is compressed from 1.370 Å to 1.355 Å, and the H–O bond length is 2.444 Å (Fig. 4). The change of bond length is in agreement with the conclusions from the change density in Fig. 5.

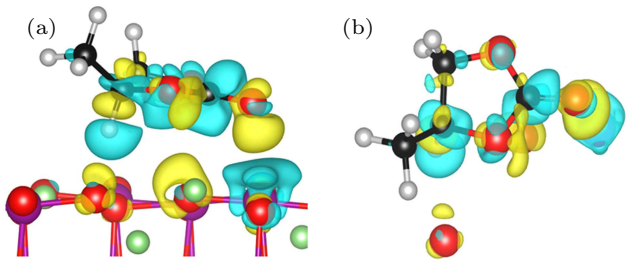


Fig. 5. Side view (a) and top view (b) of the differential charge density $\rho_{diff} = \rho_{total} - \rho_{surface} - \rho_{PC}$ plot (0.05 e/Å^3) of PC molecule adsorbed on $LiMn_2O_4$ (100) surface. The yellow regions indicate increased electron density, and blue regions represent decreased electron density.

To further disclose the origin of the change in electron density before and after adsorption, figure 6 shows the projected density of states (PDOS) for the 2p orbital of O_c atoms of PC molecule before and after adsorption. Figure 7 shows the PDOS for the d_{z^2} component of the e_g orbital of surface Mn atom which interacts with O_c before and after adsorption. As illustrated in Fig. 6, the O_c-2p level is shifted to the lower energy, which shows that the O_c of the PC molecule is stabilized, resulting in a weakened interaction between C_1 and O_c, thus the C_1–O_c bond length is stretched from 1.205 Å to 1.219 Å. Next, we analyze the electronic state of the Mn atom which interacts with O_c after adsorption. As shown in Fig. 7, the peak of the d_{z^2} component of the e_g orbital is lowered after the adsorption of the PC molecule, while the intensity of the

empty orbit above the Fermi level increases, indicating that the d_{z^2} component of the Mn^{3+} ion loses electrons. This is consistent with the previous discussion that Mn^{3+} is the donor of electrons and O_c is the acceptor of electrons. As a result, adsorbing PC molecules on the $LiMn_2O_4$ (100) surface can effectively decrease the reactivity of the Mn^{3+} ions, and thus is beneficial to suppress the disproportionated reaction of the Mn^{3+} ions on the surface. In this sense, the cycling performance of the $LiMn_2O_4$ cathode can be enhanced by using PC as the electrolyte.

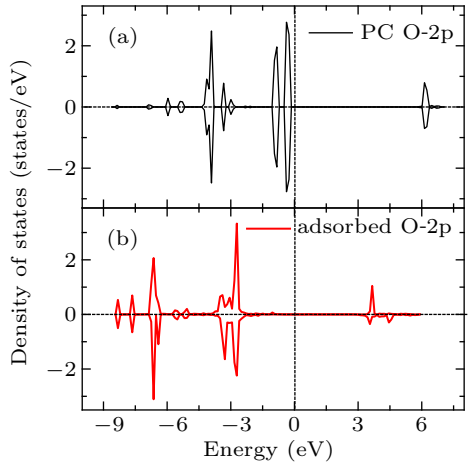


Fig. 6. The PDOS for the 2p orbital of O_c atom of PC molecule before and after adsorption.

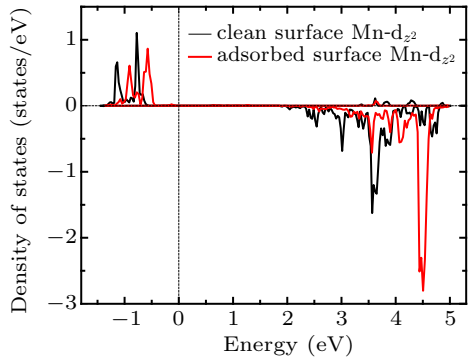


Fig. 7. The PDOS for the d_{z^2} component of the e_g orbital of Mn atom which interacts with O_c before and after adsorption.

4. Conclusions

In summary, various adsorption configurations of the propylene carbonate (PC) molecule on $LiMn_2O_4$ (100) surface have been studied base on spin-polarized DFT $+U$ calculations. The results show that the PC molecule prefers to interact with Mn atom in the $LiMn_2O_4$ (100) surface via the carbonyl oxygen (O_c), with the adsorption energy of -1.16 eV, which is an exothermic reaction. There is obvious electron transfer between adsorbed molecules and the surface during the adsorption of molecules. The d_{z^2} component of the e_g orbital of surface Mn^{3+} ion is the donor of electrons, while the 2p orbital of O_c is the acceptor of electrons, resulting in the stabilizing of the Mn^{3+} ions in the $LiMn_2O_4$ (100) surface. Our results suggest that increasing Mn coordination with O atoms at the surface by coating or molecule adsorption (such as carbonyl ad-layer, hydroxyl ad-layer, metallic oxide) can effectively inhibit the reactivity of Mn^{3+}, thereby enhance the surface stability of the Mn-based cathode material.

References

[1] Goodenough J B and Park K 2013 *J. Am. Chem. Soc.* **135** 1167
[2] Fergus J W 2010 *J. Power Sources* **195** 939
[3] Lu L G, Han X B, Li J Q, Hua J F and Ouyang M G 2013 *J. Power Sources* **226** 272
[4] Armand M and Tarascon J M 2008 *Nature* **451** 652
[5] Wu M S, Xu B and Ouyang C Y 2016 *Chin. Phys. B* **25** 018206
[6] Shi S Q, Ouyang C Y, Lei M S and Tang W H 2007 *J. Power Sources* **171** 908
[7] Moriwake H, Kuwabara A, Fisher C A J, Huang R, Hitosugi T, Ikuhara Y H, Oki H and Ikuhara Y 2013 *Adv. Mater.* **25** 618
[8] Yahia H B, Shikano M and Kobayashi H 2013 *Chem.Mater.* **25** 3687
[9] Ning F H, Li S, Xu B and Ouyang C Y 2014 *Solid State Ionics* **263** 46
[10] Ning F H, Xu B, Shi J, Wu M S, Hu Y Q and Ouyang C Y 2016 *J. Phys. Chem. C* **120** 18428
[11] Liu H, Tong Y, Kuwata N, Osawa M, Kawamura J and Ye S 2009 *J. Phys. Chem. C* **113** 20531
[12] Ouyang C Y, Shi S Q and Lei M S 2009 *J. Alloy. Compd.* **474** 370
[13] Ouyang C Y, Du Y L, Shi S Q and Lei M S 2009 *Phys. Lett. A* **373** 2796
[14] Ouyang C Y, Shi S Q, Wang Z X, Li H, Huang X J and Chen L Q 2004 *Europhys. Lett.* **67** 28
[15] Ouyang C Y, Zeng X M, S?ljivancanin Z and Baldereschi A 2010 *J. Phys. Chem. C* **114** 4756
[16] Xiao L, Xiao J, Yu X, Yan P, Zheng J, Engelhard M, Bhattacharya P, Wang C, Yang X Q and Zhang J G 2015 *Nano Energy* **16** 143
[17] Wang Z Q, Chen Y C and Ouyang C Y 2014 *Phys. Lett. A* **378** 2449
[18] Xiao R J, Li H and Chen L Q 2012 *Chem. Mater.* **24** 4242
[19] Shi S Q, Liu L J, Ouyang C Y, Wang D S, Wang Z Q, Chen L Q and Huang X J 2003 *Phys. Rev. B* **68** 195108
[20] Ouyang C Y, Shi S Q, Wang Z X, Huang X J and Chen L Q 2004 *Phys. Rev. B* **69** 104303
[21] Takahashi M, Tobishima S, Takei K and Sakurai Y 2002 *Solid State Ionics* **148** 283
[22] Zhang H, Tang Y H, Shen J Q, Xin X G, Cui L X, Chen L J, Ouyang C Y, Shi S Q and Chen L Q 2011 *Appl. Phys. A* **104** 529
[23] Chen Y C, Xie K, Pan Y, Zheng C M and Wang H L 2011 *Chin. Phys. B* **20** 28201
[24] Lee M J, Lee S, Oh P, Kim Y and Cho J 2014 *Nano Lett.* **14** 993
[25] Zhang Z F, Chen Z L, Wang G J, Ren H, Pan M, Xiao L L, Wu K C, Zhao L T, Yang J Q, Wu Q G, Shu J, Wang D J, Zhang H L, Huo N and Li J 2016 *Phys. Chem. Chem. Phys.* **18** 6893
[26] Liu W W, Wang D, Wang Z F, Deng J G, Lau W and Zhang Y N 2017 *Phys. Chem. Chem. Phys.* **19** 6481
[27] Komaba S, Kaplan B, Ohtsuka T, Kataoka Y, Kumagai N and Groult H 2003 *J. Power Sources* **119–121** 378
[28] Leggesse E G, Tsau K, Liu Y, Nachimuthu S and Jiang J 2016 *Electrochim. Acta* **210** 61
[29] Han Z H, Jia X Z, Zhan H and Zhou Y H 2013 *Electrochim. Acta* **114** 772
[30] Zhou F, Cococcioni M, Marianetti C A, Morgan D and Ceder G 2004 *Phys. Rev. B* **70** 235121
[31] Hautier G, Ong S P, Jain A, Moore C J and Ceder G 2012 *Phys. Rev. B* **85** 155208
[32] Shi S Q, Gao J, Liu Y, Zhao Y, Wu Q, Ju W W, Ouyang C Y and Xiao R J 2016 *Chin. Phys. B* **25** 18212
[33] Morgan B J and Watson G W 2007 *Surf. Sci.* **601** 5034
[34] Hu W, Wang H W, Luo W W, Xu B and Ouyang C Y 2020 *Solid State Ionics* **347** 115257
[35] Ouyang C Y, Šljivančanin Ž and Baldereschi A 2010 *J. Chem. Phys.* **133** 204701
[36] Shi Y S, Zhu S M, Zhu C L, Li Y, Chen Z X and Zhang D 2015 *Electrochim. Acta* **154** 17